Impulsive thrust collision avoidance for long-term space encounters

Matthieu Masson, Christian Artigues, Denis Arzelier, Fabrizio Dabbene, Mioara Joldeş, Martina Mammarella, Federica Paganelli Azza

Impulsive thrust collision avoidance for long-term space encounters

Matthieu Masson[1], Christian Artigues[1], Denis Arzelier[1], Fabrizio Dabbene[2], Mioara Joldes[1], Martina Mammarella[2], Federica Paganelli Azza[3] [*]

Abstract

This paper investigates how chance-constrained optimization techniques can be applied to the problem of collision avoidance between an active satellite and a passive space debris. The goal is to minimize the fuel consumption needed to perform evasive maneuvers reducing the collision probability below a given threshold. Specifically, we focus on the *long-term collision avoidance* problem and we propose two different methods, i.e., a scenario approach and a novel direct convex relaxation approach, to optimize the avoidance maneuvers while enforcing constraints on the cumulative probability of collision. The performances of these approaches are compared with a risk-selection method, and the results highlight that the direct approach is competitive with the existing methods for long-term encounters while the scenario-based method is promising for future applications in the field of spacecraft collision avoidance.

Keywords: Aerospace, Collision avoidance maneuver, Optimization, Uncertain systems

1 Introduction

The rapid expansion of human activity in space raises multiple concerns, mainly related to the accumulation of space debris and the impelling need to establish some "norms of behavior" for satellite Collision Avoidance Maneuvers (CAM), as discussed in [1]. According to the Space debris mitigation

[*]This work was not supported by any organization

[†1] M. Masson, C. Artigues, D. Arzelier, and M. Joldes are with the LAAS-CNRS laboratory, Toulouse, France.

[‡2] F. Dabbene and M. Mammarella are with the CNR-IEIIT, Torino, Italy.

[§3] F. Paganelli Azza is with AIKO S.r.l., Torino, Italy.

guidelines [2], during the operational (launch, mission and disposal) phases of spacecraft, the probability of accidental collision with known objects during the orbital lifetime should be estimated and limited, and whenever a potential collision is detected from available orbital data, on-orbit avoidance maneuvers should be considered.

The uncertain nature of the data collected to assess the risk of a collision has urged the Owners/Operators of space assets to rely on the probability of collision as the main parameter of decision. When its value is above some tolerance threshold (typically 0.001 or 0.0001), a plan of evasive maneuvers has to be decided and performed. However, the nature of the forthcoming conjunction has to be precisely characterized in order to design the most relevant series of maneuvers. Two main models — the short-term and the long-term encounters — have been widely accepted and utilized in the field of Space Situational Awareness [3].

The long-term encounter model, studied in this paper, is classically defined in the literature as an encounter between two Residents Space Objects (RSOs) for which the time interval of close approach is significant enough when compared to their corresponding orbital periods [4], [5]. Typically, long-term encounters occur at low relative velocity, inducing an additional complexity for the risk evaluation used in the CAM computation. Moreover, unlike the so-called short-term encounters [6], the relative motion during the conjunction can no longer be assumed to be rectilinear (a straight line) and the event is not supposed to be instantaneous.

If several approaches for the systematic synthesis of CAM exist for the wider class of short-term encounters, the literature is relatively poor concerning the other class. Indeed, one may mention the references [7] and [8] which end up respectively with a linear programming and a mixed integer linear programming formulation of different kinds of collision avoidance problems. In particular, the last reference recasts the CAM problem as a chance-constrained fuel minimization problem and replaces the cumulative (or joint) non collision constraint by a conjunction of individual constraints based on instantaneous collision probabilities enforced on a time grid. Finally, the authors use a risk selection relaxation to obtain a deterministic mixed integer linear programming problem solved by a classical big-M technique.

Starting from this same initial setting for the CAM problem, we propose, first, a new direct approach that allows to circumvent the conservative risk selection convexification by computing explicit expressions of the probabilistic constraints and of their gradients. This result is obtained at the expense of a well-chosen polyhedral approximation of the forbidden region.

The obtained CAM problem can then be tackled with standard numerical tools of convex optimization. Secondly, the standard scenario approach [9] is applied to the selected problem by sampling also the time parameter and properly convexifying the collision avoidance region using a rotating hyperplane tangent to the forbidden region.

Notation Given integers $a \leq b$, we denote by $[\![a, b]\!]$ the set of integers $\{a, \ldots, b\}$. The function $\mathrm{erf}(x) = \frac{2}{\sqrt{\pi}} \int_0^x e^{-s^2} \mathrm{d}s$ defines the Gauss error function while the function

$$\mathbb{1}_{t \geq t_1}(t) = \begin{cases} 0 & \text{if} \quad t < t_1 \\ 1 & \text{if} \quad t \geq t_1 \end{cases}$$

is the indicator function of the subset $[t_1, +\infty)$.

2 A chance-constrained formulation of the impulsive collision avoidance problem

2.1 Linearized orbital dynamics for long-term encounters

This section focuses on the mathematical description of the framework related to a (possible) encounter between an active satellite, called *primary* (p), and a (passive) debris, called *secondary* (s), over a time interval $\mathcal{I} = [\underline{t}, \bar{t}]$.

Formally, to describe the dynamics of the two RSOs during the maneuver, the following simplifying assumption is made.

Assumption 1 (Linearized relative dynamics) *During the time interval $\mathcal{I}$ defining the encounter, the relative distance between p and s with respect to a given reference orbit is small compared with their respective distance to Earth.*

Assuming that the ballistic motion of the two RSOs is Keplerian, their equations of motion can be linearized around the Keplerian primary's reference orbit, and formulated via the usual Cartesian coordinates in a moving Local Vertical Local Horizontal (LVLH) orbital frame centered in the primary object, rotating with its angular velocity and such that the z-axis points towards Earth, the y-axis is orthogonal to the orbital plane and opposite to the angular moment, and the x-axis completes the right-hand triad [10].

The set of linearized equations of motion are known as the standard Tschauner-Hempel (or Lawden) equations [11], with the corresponding Yamanaka-Ankersen's state transition matrix [12] for elliptic orbits.

Let us consider the state vector $X_{p/s}(t) \in \mathbb{R}^6$, containing the position $r_{p/s}(t) \in \mathbb{R}^3$ and velocity $v_{p/s}(t) \in \mathbb{R}^3$ of the primary (or secondary) body in the LVLH frame, and let us introduce the state transition matrix $\Phi(\cdot,\cdot)$. Then, the orbital dynamics of the secondary body can be defined as

$$X_s(t) = \Phi(t,\underline{t})\underline{X}_s, \tag{1}$$

where $\underline{X}_s \doteq X_s(\underline{t})$ is the initial condition for the secondary.

Unlike the secondary, the primary is actuated and can use a high-thrust propulsion to modify its trajectory. We rely on the following assumption [13] to define its orbital dynamics.

Assumption 2 (Impulsive approximation of high-thrust) *The primary satellite performs impulsive maneuvers, relying on a high-thrust propulsion system, generating at pre-specified time instants $t_i \in \mathcal{I}$ an instantaneous velocity increment $\Delta V_i \in \mathbb{R}^3$ expressed in the LVLH frame, assuming that 6 orthogonal thrusters are aligned to the LVLH frame axis [14], such that the primary orbital dynamics over the time interval $\mathcal{I}$ can be formulated as*

$$X_p(t_i^+) = X_p(t_i^-) + B_1\Delta V_i, \text{ with } B_1 = \begin{bmatrix} 0_{3\times 3} & \mathbb{I}_3 \end{bmatrix}^T.$$

Let us assume that m impulsive evasive maneuvers are performed at the instants $\underline{t} \le t_1 \le \cdots t_i \le \cdots t_m \le \bar{t}$. Then, for a given $t \in \mathcal{I}$ and after k maneuvers, the state vector of the primary can be defined as typically done in the rendezvous framework (see e.g., [8], [15]) by:

$$X_p(t) = \Phi(t,\underline{t})\underline{X}_p + \sum_{i\in\{1,\ldots,k\}} \Phi(t,t_i)B_1\Delta V_i, \tag{2}$$

where t is such that $\underline{t} \le t_k \le t \le t_{k+1} \le t_m = \bar{t}$.

As discussed later on, the definition of the collision involves the relative position $r(t)$ of the primary p with respect to the secondary s. It is therefore natural to express their relative state vector in terms of the transition matrix and of the sequence of m impulsive controls as follows

$$X(t) = X_p(t) - X_s(t) = \Phi(t,\underline{t})\underline{X} + C(t)\Delta V, \tag{3}$$

with $\underline{X} \doteq X(\underline{t})$, $\Delta V = [\Delta V_1^T \ \ldots \ \Delta V_m^T]^T$ and

$$C(t) = [\mathbb{1}_{t\ge t_1}(t)\Phi(t,t_1)B_1 \ \ldots \ \mathbb{1}_{t\ge t_m}(t)\Phi(t,t_m)B_1].$$

Even though the dynamics of p and s are assumed to be perfectly known, various sources of inaccuracies (e.g., limitations of the ground-based sensors and of the orbital propagators, neglected orbital perturbations) prevent a perfect prediction of their state kinematic vectors at time $\underline{t}$. A usual way to partially capture this uncertainty is to assume that the initial state vectors $\left(\underline{X}_p \doteq X_p(\underline{t}),\, \underline{X}_s \doteq X_s(\underline{t})\right)$ follow independent 6-dimensional Gaussian distributions, i.e., $\underline{X}_{p/s} \sim \mathcal{N}_6(\mu_{\underline{X}_{p/s}}, \Sigma_{\underline{X}_{p/s}})$ [16]. Then, from Assumption 1 it follows that $\forall\ t \in \mathcal{I}$, $X_p(t)$ and $X_s(t)$ are Gaussian vectors:

$$\begin{aligned} X_p(t) &\sim \mathcal{N}_6(\mu_{X_p}(t), \Sigma_{X_p}(t)), \\ X_s(t) &\sim \mathcal{N}_6(\mu_{X_s}(t), \Sigma_{X_s}(t)), \end{aligned} \tag{4}$$

with mean vectors and covariance matrices given by

$$\begin{aligned} \mu_{X_p}(t) &= \Phi(t,\underline{t})\mu_{\underline{X}_p} + C(t)\Delta V, \\ \mu_{X_s}(t) &= \Phi(t,\underline{t})\mu_{\underline{X}_s}, \\ \Sigma_{X_p}(t) &= \Phi(t,\underline{t})\Sigma_{\underline{X}_p}\Phi(t,\underline{t})^T, \\ \Sigma_{X_s}(t) &= \Phi(t,\underline{t})\Sigma_{\underline{X}_s}\Phi(t,\underline{t})^T. \end{aligned} \tag{5}$$

As a consequence, the relative state vector $X(t)$ is also a Gaussian vector $X(t) \sim \mathcal{N}_6(\mu_X(t), \Sigma_X(t))$ with mean value $\mu_X(t) = \mu_{X_p}(t) - \mu_{X_s}(t)$ and covariance matrix $\Sigma_X(t) = \Sigma_{X_p}(t) + \Sigma_{X_s}(t)$. Analogously, the relative position vector $r(t)$ is defined by a Gaussian vector as

$$\begin{aligned} r(t) &\sim \mathcal{N}_3(\mu_r(t), \Sigma_r(t)), \\ \mu_r(t) &= B_2\mu_X(t), \\ \Sigma_r(t) &= B_2\Sigma_X(t)B_2^T, \end{aligned} \tag{6}$$

with $B_2 = \begin{bmatrix} \mathbb{I}_3 & 0_{3\times 3} \end{bmatrix}$.

2.2 Probabilistic characterization of the collision

Checking *a priori* if a collision occurs at a certain time t requires a geometrical criterion based on the shape and the orientation of both p and s. First, we state a conservative but standard assumption [16, 3] that enables us to neglect the attitude (orientation) of both objects.

Assumption 3 (Spherical bodies [3]) *Both the primary and the secondary's shape are approximated by spheres of known radius R_p and R_s, respectively.*

Remark 1 *Note that Assumption 3 is usually necessary also because the geometry of s is often poorly known.*

Based on Assumption 3, we can introduce a first general definition of a collision between p and s.

Definition 1 (Collision) *A collision between the primary body p and the secondary body s occurs in the interval of interest $\mathcal{I}$ if there exists a time $t \in \mathcal{I}$ such that their relative distance $r(t)$ is lower than the so-called hardbody radius, defined as $R_c = R_p + R_s$, i.e., $\|r(t)\|_2 \leq R_c$.*

From Definition 1 and given the stochastic characterization of the relative vector $r(t)$ in (6), we have that the collision event considered in this framework is a random event characterized as such by a probability of collision.The objective is to optimize the sequence of impulsive maneuvers while upper-bounding the probability of collision or, equivalently, enforcing a constraint on the collision probability for the primary object to stay below a given threshold ε. Such constraint can be captured by chance constraints of the form

$$\mathcal{P}\Big(\sup_{t\in\mathcal{I}} g(t, \Delta V, \underline{X}) \geq 0\Big) \leq \varepsilon, \tag{7}$$

with $g(t, \Delta V, \underline{X}) \doteq R_c^2 - \|r(t)\|_2^2$. Let us now introduce the concept of forbidden region.

Definition 2 (Forbidden region) *For a selected time interval $\mathcal{I}$, the forbidden region $\mathcal{V}$ is defined as the set of initial conditions $\underline{X}$ leading to a collision for some $t \in \mathcal{I}$, i.e.,*

$$\mathcal{V} = \left\{\underline{X} \in \mathbb{R}^6 \,|\, \exists t \in \mathcal{I} \text{ such that } \|r(t)\|_2^2 \leq R_c^2\right\}. \tag{8}$$

From Definition 2, the chance constraint (7) becomes:

$$\mathcal{P}_c \doteq \mathcal{P}\left(\underline{X} \in \mathcal{V}\right) = \int_{\mathcal{V}} \mathcal{N}_6\left(\underline{X}; \mu_{\underline{X}}, \Sigma_{\underline{X}}\right) \mathrm{d}\underline{X} \leq \varepsilon. \tag{9}$$

The probability $\mathcal{P}_c$ is known as *the cumulative collision probability* [17], which can be reformulated as a 3D integral under few restrictive assumptions on the encounter as detailed in [16], and by relaxing the most stringent assumptions involved in the classical short-term formulation (see e.g., [3], [5], [18]).

Remark 2 *Note that the formulations* (9) *and* (7) *are equivalent and both will be used thereafter to describe the non-collision constraint.*

2.3 The collision avoidance optimization problem

In this section, we define the collision avoidance problem as a chance-constrained optimization problem. When designing a collision avoidance maneuver, several factors come into play. The reduction of fuel consumption is of paramount importance in order to extend as far as possible the operational lifetime of the active asset.

Assuming 6 ungimbaled impulsive thrusters rigidly mounted on each face of the primary, the fuel consumption required to perform m evasive maneuvers is defined as in [19] by the 1-norm of ΔV, i.e.,

$$J = \sum_{i=1}^{m} \|\Delta V_i\|_1. \tag{10}$$

This will be the cost function of the chance-constrained optimization problem. Moreover, we have to consider the degradation of the mission due to the correction maneuvers since they will force the primary object to leave its reference orbit. For this reason, a return of the primary to its Keplerian orbit at the end of the time interval $\mathcal{I}$ [8] is imposed as an additional constraint of the control design problem. Hence, the collision avoidance problem is restated as a minimum-fuel chance-constrained optimization problem:

$$\begin{aligned} \min_{\Delta V_i} \quad & \sum_{i=1}^{m} \|\Delta V_i\|_1 \\ \text{s.t.} \quad & \mathcal{P}\left(\underline{X} \in \mathcal{V}\right) \leq \varepsilon, && \text{(11a)} \\ & \mu_{X_p}(\bar{t}) = 0. && \text{(11b)} \end{aligned}$$

Remark 3 *As previously mentioned, the chance constraints involved in Problem* (11) *can be equivalently reformulated using* (7)*. Consequently, we can rewrite Problem* (11) *as follows*

$$\begin{aligned} \min_{\Delta V_i} \quad & \sum_{i=1}^{m} \|\Delta V_i\|_1 \\ s.t. \quad & \mathcal{P}\Big(\sup_{t\in\mathcal{I}} g(t, \Delta V, \underline{X}) \geq 0\Big) \leq \varepsilon, \\ & \mu_{X_p}(\bar{t}) = 0. \end{aligned} \tag{12}$$

In Problem (11), $\mathcal{V}$ and μ_{X_p} depend on the relative position vector $r(t)$ and, given (2)–(6), they also depend on ΔV_i, $i \in [\![1, m]\!]$, which are the

decision variables of the optimization problem. We notice that the constraint (11b) is an affine equality constraint with respect to the decision variables ΔV_i, $i \in [\![1, m]\!]$. In addition, unlike constraint (11b), the chance constraint (11a) bounding the risk of collision is in general difficult to evaluate and optimize against, without any simplifying assumptions. This is mainly due to the joint nature of the chance constraints (11a) compared to individual probabilistic constraints [20].

Moreover, the computation of $\mathcal{P}_c$ as a function of the control variables $\Delta V_i, i \in [\![1, m]\!]$ is still an open problem. Typically, the computation of $\mathcal{P}_c$ can be performed *via* Monte-Carlo simulations, by propagating the relative trajectories and checking if a collision occurs during the encounter. However, this method is computationally expensive and, without any additional assumption concerning the encounter, there exists no closed-form to assess the value of $\mathcal{P}_c$. In particular, the computational burden is extremely heavy because these methods rely on high-order quadrature for the evaluation of multi-dimensional integrals. Additionally, the numerical computation depends on the underlying assumptions on the dynamics as described in [16] or on the distribution laws. In the next section, different approximations of Problem (11), for which efficient numerical solutions are available, are proposed.

3 Approximated solutions for the collision avoidance problem

Two approaches to approximate the solution of Problem (11) are presented. Firstly, a novel method called *direct convex relaxation* replaces the probabilistic constraint defining $\mathcal{P}_c$ by the *instantaneous collision probability* [3] and computes in closed-form the gradient of the new probability with respect to the decision variables ΔV_i. Secondly, we present an application of the well-known scenario approach [21] to the context of collision avoidance maneuvers, thus providing probabilistic guarantees to the solution of the chance-constrained optimization problem.

3.1 Direct convex relaxation of collision probability

A simple way to tackle joint chance constraints in Problem (11) is to enforce pointwise-in-time probability constraints by replacing the cumulative collision probability with the *instantaneous collision probability* [3], which is a lower bound for the cumulative collision probability [17, 22]. It is defined as

the probability $\mathcal{P}_i(t)$ that a collision occurs at a given instant $t \in \mathcal{I}$. Consequently, the new individual chance constraints involving the instantaneous collision probability are

$$\mathcal{P}_i(t) = \mathcal{P}\left(\|r(t)\|_2 \leq R_c\right) \leq \varepsilon', \ \forall\ t \in \mathcal{I}, \tag{13}$$

where the computation of $\mathcal{P}_i(t)$, for each given $t \in \mathcal{I}$, can be reduced to the integration of a three-dimensional Gaussian density over the hardbody sphere as in [3]. Efficient numerical methods have been recently proposed to compute this integral (see e.g., [23], [24], and references therein). This approximation has already been used in [8] where a risk selection approach [25] was applied to a similar collision avoidance problem. Moreover, in practice, we set the threshold $\varepsilon' = \varepsilon/(\bar{t} - \underline{t})$.

Remark 4 *It is important to highlight that the new individual chance constraints* (13) *do not guarantee the satisfaction of the original joint chance constraint* (9) *even though their number is infinite. To be numerically tractable, only a finite number of individual instantaneous constraints* (13) *will be enforced on a pre-specified time grid of N time instants, i.e.,* $\underline{t} < \hat{t}_1 < \cdots < \hat{t}_{N-1} < \bar{t}, N \in \mathbb{N}^\star$.

In the approach we propose in this paper, in order to get differential constraints for which analytical expressions of the instantaneous constraint and of its gradient are available, the geometry of the hardbody is slightly modified.

Assumption 4 (Polyhedral approximation of the hardbody) *The spherical hardbody is approximated by a cubic polyhedron* $\Xi(t)$ *centered at the origin and containing* $\mathcal{B}(0, R_c)$*, with faces normal to the eigendirections of* $\Sigma_r(t)$.

Since $\mathcal{B}(0, R_c) \subset \Xi(t)$, this approximation is conservative and consequently $\forall k \in [\![1, N]\!]$ we have that

$$\mathcal{P}(r(\hat{t}_k) \in \Xi(\hat{t}_k)) \leq \varepsilon' \Rightarrow \mathcal{P}_i(\hat{t}_k) \leq \varepsilon'.$$

Then, the new chance-constrained optimization problem is

$$\begin{aligned} \min_{\Delta V_i} \quad & \sum_{i=1}^{m} \|\Delta V_i\|_1 \\ \text{s.t.} \quad & \mathcal{P}_i(\hat{t}_k) \leq \varepsilon', \quad k \in [\![1, N]\!], \\ & \mu_{X_p}(\bar{t}) = 0. \end{aligned} \tag{14}$$

Remark 5 *The motivation to choose such an approximation is twofold. First, due to the separability and linearity properties of the individual chance constraints, Problem* (14) *is a smooth convex optimization problem, which can be solved using efficient numerical tools [26]. Secondly, this approximation allows us to derive an analytical expression of the collision probability and of its gradient with respect to the decision variables* ΔV_i*. Indeed, for* $k \in [\![1, N]\!]$*, let* σ_l^2 *(*$l = 1, 2, 3$*), be the eigenvalues of* $\Sigma_r(\hat{t}_k)$*, and let* P_k *be the transformation matrix to the orthogonal frame, composed of corresponding eigenvectors with unit norm. Then, at any time* $\hat{t}_k$*,* $k \in [\![1, N]\!]$*, the random vector* $Y_k = P_k r(\hat{t}_k)$ *follows a Gaussian law, whose mean and covariance matrix are* $\mu_{Y_k} = P_k \mu_{r(\hat{t}_k)}$ *and* $\Sigma_{Y_k} = P_k \Sigma_{r(\hat{t}_k)} P_k^T$*, respectively. Hence, the linear separable chance constraints* $\mathcal{P}_i(\hat{t}_k) \leq \varepsilon'$*,* $k \in [\![1, N]\!]$ *are equivalently redefined as*

$$\mathcal{P}\left(Y_k \in [-R_c, R_c]^3\right) \leq \varepsilon', \quad k \in [\![1, N]\!], \tag{15}$$

where the probability $\mathcal{P}\left(Y_k \in [-R_c, R_c]^3\right)$, with respect to the l-th components $\mu_{Y_k}^{(l)}$ of μ_{Y_k} (with $l \in [\![1, 3]\!]$) is given by

$$\begin{aligned}
&\mathcal{P}\left(Y_k \in [-R_c, R_c]^3\right) \\
&= \frac{(2\pi)^{-\frac{3}{2}}}{\prod_{l=1}^{3} \sigma_l} \int_{-R_c}^{+R_c} \int_{-R_c}^{+R_c} \int_{-R_c}^{+R_c} \exp\left(-\sum_{l=1}^{3} \frac{(y_l - \mu_{Y_k}^{(l)})^2}{2\sigma_l^2}\right) \mathrm{d}y_1 \mathrm{d}y_2 \mathrm{d}y_3
\end{aligned}$$

$$\begin{aligned}
&= \prod_{l=1}^{3} \frac{1}{\sqrt{2\pi}\sigma_l} \int_{-R_c}^{+R_c} \exp\left(-\frac{(y_l - \mu_{Y_k}^{(l)})^2}{2\sigma_l^2}\right) \mathrm{d}y_l \\
&= \prod_{l=1}^{3} \frac{1}{2} \left(\operatorname{erf}\left(\frac{\mu_{Y_k}^{(l)} - R_c}{\sqrt{2}\sigma_l}\right) + \operatorname{erf}\left(\frac{\mu_{Y_k}^{(l)} + R_c}{\sqrt{2}\sigma_l}\right)\right).
\end{aligned}$$

Applying the chain rule, the gradient of $\mathcal{P}\left(Y_k \in [-R_c, R_c]^3\right)$ with respect to the decision variables ΔV_i is

$$\frac{\partial \mathcal{P}\left(Y_k \in [-R_c, R_c]^3\right)}{\partial \Delta V_i} = \frac{\partial \mathcal{P}\left(Y_k \in [-R_c, R_c]^3\right)}{\partial \mu_{Y_k}} \cdot \frac{\partial \mu_{Y_k}}{\partial \Delta V_i},$$

where the partial derivative of μ_{Y_k} with respect to ΔV_i is

$$\frac{\partial \mu_{Y_k}}{\partial \Delta V_i} = \begin{cases} P_k[I_3\ 0_3]\Phi(\hat{t}_k, t_i)B & \text{if } t_i \leq \hat{t}_k, \\ 0_3 & \text{otherwise.} \end{cases} \tag{16}$$

Furthermore, for each $l \in [\![1, 3]\!]$, we have

$$\begin{aligned} &\frac{\partial}{\partial \mu_{Y_k}^{(l)}} \mathcal{P}\left(Y_k \in [-R_c, R_c]^3\right) \\ &= \frac{\exp\left(-\left(\frac{\mu_{Y_k}^{(l)} - R_c}{\sqrt{2}\sigma_l}\right)^2\right) + \exp\left(-\left(\frac{\mu_{Y_k}^{(l)} + R_c}{\sqrt{2}\sigma_l}\right)^2\right)}{\sqrt{\pi}\sigma_l\left(\operatorname{erf}\left(\frac{\mu_{Y_k}^{(l)} - R_c}{\sqrt{2}\sigma_l}\right) + \operatorname{erf}\left(\frac{\mu_{Y_k}^{(l)} + R_c}{\sqrt{2}\sigma_l}\right)\right)} \cdot \\ &\cdot \sqrt{2}\mathcal{P}\left(Y_k \in [-R_c, R_c]^3\right). \end{aligned} \tag{17}$$

In this way, we obtain a convex optimization problem characterized by a particular cubic polyhedral approximation, which can be solved using standard numerical tools.

3.2 Scenario-based collision probability

The scenario optimization approach has been introduced in [9, 21] to solve robust or chance-constrained optimization problems in which constraints are imprecisely known. In particular, it presumes a probabilistic description of the uncertainty characterized through a set Δ describing the set of admissible situations, and a probability $\mathcal{P}$ over Δ. Then, the scenario approach allows to obtain a convex optimization problem where the initial chance constraints are replaced by deterministic constraints for a set of *scenarios* $\boldsymbol{\delta} = \{\delta^{(1)}, \ldots, \delta^{(N_s)}\} \in \Delta^{N_s}$, where each of the N_s scenarios is independently extracted from the probability measure $\mathcal{P}_\Delta$. In detail, given an uncertainty set Δ, if $\mathcal{P}_\Delta$ is the probability on Δ and $\varepsilon \in (0, 1)$ is an acceptable risk of constraint violation, the uncertain chance-constrained problem is defined as

$$\begin{aligned} \min_{x \in \mathcal{X}} \quad & c^T x \\ \text{s.t.} \quad & \mathcal{P}\Big(f(x, \delta) > 0\Big) \leq \varepsilon, \quad \delta \in \Delta, \end{aligned} \tag{18}$$

where $x \in \mathcal{X}$ is the optimization variable, $\mathcal{X}$ is a compact and convex set, and the function $f(x, \delta) : \mathcal{X} \times \Delta \to \mathbb{R}$ is convex in x for all $\delta \in \Delta$. The scenario approach aims at redefining the uncertain problem as a deterministic

problem taking into account only a finite set of N_s constraints, randomly chosen among the possible constraint instances of the uncertain problem. In this way, it is possible to bound the probability of the original constraints that are possibly violated by the randomized solution. Formally, the scenario problem is stated as follows.

Definition 3 (Scenario problem) *Given the violation level $\varepsilon \in (0,1)$ and the confidence level $\beta \in (0,1)$, if one extracts (at least) N_s i.i.d. samples $\delta^{(1)}, \ldots, \delta^{(N_s)}$ according to probability $\mathcal{P}_\Delta$ such that*

$$\sum_{\ell=1}^{d} \binom{N_s}{\ell} \varepsilon^{\ell}(1-\varepsilon)^{N_s-\ell} \leq \beta, \tag{19}$$

where d is the number of optimization variables, then under some technical assumptions and under the convexity of the constraint $f(x,\delta)$ in x for given δ, the condition

$$\mathcal{P}\Big(f(x,\delta) \leq 0\Big) \geq 1-\varepsilon,$$

holds with probability no smaller than $1-\beta$.

In this specific case study, the only random variable is the initial condition $\underline{X} \sim \mathcal{N}_6(\mu_{\underline{X}}, \Sigma_{\underline{X}})$. However, choosing $\underline{X}$ as the uncertain parameter δ would yield joint constraints with complex feasible sets: for a given initial state there exists no closed form characterizing the set of all the ΔV leading to no collision during the whole encounter. Nevertheless, we know that requiring the same condition for a given instant leads to pointwise-in-time constraints [27], which are more tractable.

Then, we can observe that the scenario approach presented in [21] is distribution-free, i.e., the result applies independently of the distribution of the uncertain parameter. Based on those observations, we choose to *randomize* also the time parameter by setting $\delta = [\underline{X}^T \ \mathcal{T}]^T$, where $\mathcal{T}$ is a uniformly distributed random variable valued in $\mathcal{I}$, i.e. $\mathcal{T} \in \mathcal{U}(\mathcal{I})$ ($\mathcal{T}$ and $\underline{X}$ are assumed to be independent). Consequently, using the function g defined in (7), the new chance constraint related to the probability of collision is given as

$$\mathcal{P}_\Delta\left(g(\mathcal{T}, \Delta V, \underline{X}) < 0\right) \geq 1-\varepsilon. \tag{20}$$

Remark 6 *The satisfaction of the non collision constraint* (20) *does not guarantee the satisfaction of the original joint chance constraint* (12)*, since the two constraints rely on different constraint functions and different probability distributions.*

Therefore, the new chance-constrained optimization problem is formulated as follows

$$
\begin{aligned}
\min_{\Delta V_i} \quad & \sum_{i=1}^{m} \|\Delta V_i\|_1 \\
\text{s.t.} \quad & \mathcal{P}_{\Delta}\left(g(\mathcal{T}, \Delta V, \underline{X}) < 0\right) \geq 1 - \varepsilon, \\
& \mu_{X_p}(\bar{t}) = 0.
\end{aligned} \tag{21}
$$

The next step consists in convexifying the constraint (20) to properly apply the scenario approach to Problem (21).

In the collision avoidance literature, a classical convexification method consists in building an inner approximation of the feasible set based on a hyperplane tangent to the forbidden region. This implies that, for each constraint, the choice of the tangent hyperplane must be consistent with the dynamics of the problem. For instance, in rendezvous problems with obstacle collision avoidance model predictive control strategies usually rely on a rotating hyperplane to ensure that the chaser circumvent the obstacle and reach the target (see e.g., [28]–[29] and references therein). However, the majority of these methods rely on an stringent assumption on the constant rate of the rotating hyperplane, which is not applicable in the case study described in this paper. Indeed, we rely on the assumption that both primary and secondary objects remain close to the reference orbit of the primary, and therefore we propose a relaxation approach based on the construction of a hyperplane related to the Keplerian orbit.

Assumption 5 *The constraint* (20)*, which can be defined in terms of the relative position vector as*

$$\|r(\Delta V, \underline{X}, \mathcal{T})\|_2^2 > R_c^2,$$

with

$$r(\Delta V, \underline{X}, \mathcal{T}) = B_2\Big(\Phi(\mathcal{T}, \underline{t})\underline{X} + C(\mathcal{T})\Delta V\Big),$$

is conservatively reformulated as $n^T r(\Delta V, \underline{X}, \mathcal{T}) - R_c > 0$*, where* $n = \frac{r_{ref}}{\|r_{ref}\|_2}$*, and* $r_{ref} = B_2\Phi(\mathcal{T}, \underline{t})\underline{X}$ *is the relative position vector associated with the reference orbit.*

Then, based on Assumption 5, we can finally reformulate Problem (21)

as a scenario optimization problem as follows

$$\min_{\Delta V} \quad \sum_{i=1}^{m} \|\Delta V_i\|_1 \tag{22a}$$

$$\text{s.t.} \quad n_{(\ell)}^T r(\Delta V, \underline{X}^{(\ell)}, t^{(\ell)}) - R_c > 0, \quad \ell \in [[1, N_s]], \tag{22b}$$

where we can guarantee that

$$\mathcal{P}_\Delta \left(g(\mathcal{T}, \Delta V, \underline{X}) < 0 \right) \geq 1 - \varepsilon,$$

with probability not smaller than $1 - \beta$, if we extract N_s samples $(\underline{X}, \mathcal{T})^{(\ell)}$ from $\mathcal{P}_\Delta$, with $\Delta = [\mathcal{N}_6(\mu_{\underline{X}}, \Sigma_{\underline{X}}), \mathcal{U}(\mathcal{I})]$.

4 Numerical results

The algorithms are tested on two case studies borrowed from [17] (case #1 and case #9) with mean values and covariance matrices expressed at the Time of Closest Approach (TCA). Their performances are compared with those obtained by the risk selection approach proposed in [8] with $M = 10^4$ (i.e., big-M constant in the Mixed-Integer Linear Programming problem). The simulations were performed on Matlab R2021b® with a 12th Gen Intel®Core(™) i5-1235U 1.30 GHz and 16 GB of RAM. The risk selection model and the scenario approach were built using Gurobi 11.0.0, whereas the direct approach problem was solved by the SQP algorithm of the *fmincon* Matlab(™) function with a maximum of 10^4 iterations and an initial point chosen after a trial and error procedure. For the whole numerical study, the maximal number of possible maneuvers in each direction is set to $m = 5,\ 10,\ 20$ (evenly spaced in $\mathcal{I}$, i.e. $t_i = \underline{t} + (i-1)\frac{\bar{t}-\underline{t}}{m-1}, i \in [\![1, m]\!]$). Similarly, the number of discretization times for a given N is defined as $\hat{t}_k = \underline{t} + k\frac{\bar{t}-\underline{t}}{(N+1)}, k \in [\![1, N]\!]$[1] for N given for each example. By their very nature, the results obtained from each run of the scenario algorithm may vary significantly. Therefore, we chose to select the best result (in terms of fuel consumption) out of 5 successive runs. For the three methods, ΔV components with magnitude lower than 1e-5 m/s have been set to zero. Given each maneuvers plan, a table presenting the obtained approximation $\overline{J}$ of $J^\star \doteq \|\Delta V^\star\|_1$, the maximum of the *instantaneous collision probability* $\mathcal{P}_i^{max}$ using the algorithm described in [23] and finally, an approximation $\tilde{\mathcal{P}}_c$ of the cumulative collision probability $\mathcal{P}_c$, obtained via a Monte-Carlo

[1] For numerical reasons, $\underline{t}$ and $\bar{t}$ are not included in the discretization grid.

(MC) simulation sampling 1×10^8 initial conditions, is given for each test case. For convenience, the risk selection, the direct approach and the scenario will be respectively labeled 'RS', 'DIR' and 'SC' in the figures and tables proposed, whereas 'BAL' will refer to the ballistic orbit. No CPU or user times have been reported since the used optimization solvers (Gurobi 11.0.0, *fmincon*) may have computation performances hardly comparable. Still, roughly speaking, the different experiments suggest that the scenario is much more demanding in general than the two others which have similar performances.

4.1 Test case 1 (#1 case of [17])

In this test case, two satellites in geosynchronous orbits (GEO) are involved in the conjunction where the mean distance at TCA is less than the combined hardbody radius R_c and the cumulative collision probability is computed as 0.217. This collision probability is the outcome of two different intervals of accumulation: the first one $[-2,000\ s, +2,000\ s]$ is centered around the TCA while the second one is shorter and begins around 9,500 s after the TCA. The number of evenly spread time instants $\hat{t}_k, k \in [\![1, N]\!]$ is equal to $N = 500$, belonging to the encounter time interval $\mathcal{I} = [\underline{t} = -50,000\ s, \bar{t} = 50,000\ s]$, (corresponding to 0.6 orbits before and after the TCA), with a time step of $199.6s$. Regarding the scenario approach, the violation level and the confidence levels were set to $\varepsilon = 10^{-3}$ and $\beta = 10^{-3}$, respectively. The instantaneous collision probability threshold is set to $\varepsilon' = \frac{\varepsilon}{\bar{t}-\underline{t}} = 10^{-8}$.

		Methods		
# ΔV		RS	DIR	SC
$n = 5$	$\bar{J}(mm/s)$	4.77	**3.27**	5.94
	$\mathcal{P}_i^{max}$	4e-20	4e-13	0
	$\tilde{P}_c$	0	0	0
$n = 10$	$\bar{J}(mm/s)$	3.94	**3.08**	7.18
	$\mathcal{P}_i^{max}$	4e-19	1e-23	0
	$\tilde{P}_c$	0	0	0
$n = 20$	$\bar{J}(mm/s)$	3.97	**2.88**	11.88
	$\mathcal{P}_i^{max}$	4e-18	7e-11	0
	$\tilde{P}_c$	0	0	0

Table 1: Test case 1 - Fuel consumption, maximal instantaneous collision probability and MC cumulative collision probability for 5, 10 and 20 maneuvers respectively.

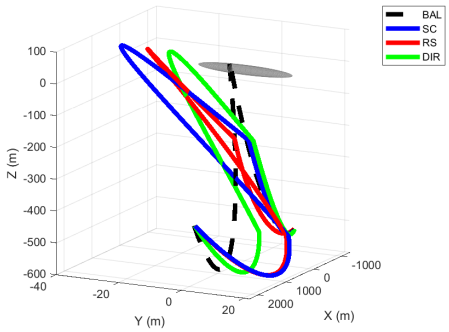

Figure 1: Test case 1 - mean relative trajectories and forbidden region (in grey) for $m = 5$.

The results reported in Table 1 show that the direct approach outperforms the two other methods for all chosen m, whereas all the methods comply with the initial risk requirement measured by $\mathcal{P}_i^{max}$ or $\tilde{\mathcal{P}}_c$.

The mean relative trajectories obtained by applying the three approaches are depicted in Fig. 1, illustrating the differences between the three avoidance strategies. This is more clearly noticeable in Figure 2, which exposes the three maneuvers plans. Each strategy is based on 4 maneuvers out of the five possible but the DIR maneuver plan only includes out-of-plane maneuvers while the RS and SC strategies are more similar (using all three thrust directions) with slight differences in the choice of the firing directions of each maneuver. Note also that the hierarchy of strategies is clearly illustrated by the mean miss-distance plot in Figure 3: the less consuming plan leading to a smaller mean miss-distance.

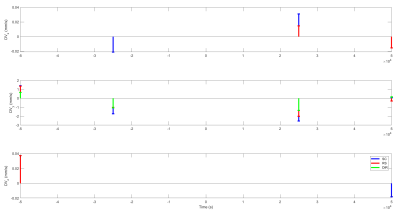

Figure 2: Test case 1 - ΔV components vs firing times for $m = 5$.

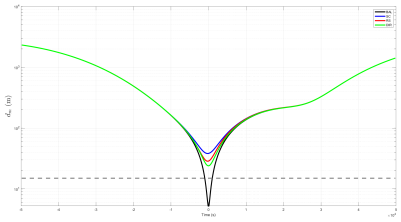

Figure 3: Test case 1 - Distances between the mean relative trajectories and the origin of the hardbody for $m = 5$; harbody radius indicated by the dotted black line.

4.2 Test case 2 (#4 case of [17])

We consider the case study number 4 in [17], which involves two satellites in geosynchronous orbits (GEO) where the mean distance at the time of closest approach (TCA) is greater than the combined hardbody radius R_c and the cumulative collision probability is approximately 7.31e-2. The main feature of this example is that the interval of accumulation of the collision probability, roughly defined as $[3,000\ s, 11,000\ s]$, is "offset-from-the-TCA". Therefore, a non symmetric encounter time interval, $\mathcal{I} = [\underline{t} = -60000\ s, \bar{t} = 120000\ s]$ has been considered for the computation of avoiding maneuvers. A number of $N = 500$ instants is used for the instantaneous collision probability constraints, with a time step of 514s and the instantaneous collision probability threshold is set to $\epsilon' = \frac{\epsilon}{\bar{t}-\underline{t}} = 2.78.10^{-09}$. For this case the violation level and the confidence levels are respectively set to $\varepsilon = 5 \times 10^{-4}$ and $\beta = 10^{-3}$.

The results reported in Table 2 and the plots of Figures 4 and 5 describe a different situation compared to the first example. The scenario approach is more efficient in general and the least expensive one for $m = 5$ and $m = 10$, proving that this approach may be a promising alternative to the existing RS approach. A noteworthy feature of these results is that all three methods give very similar avoiding maneuvers plans comprising up to 6 in-track maneuvers when $m = 10$. Probably due to the offset of the TCA with respect to the $\mathcal{P}_c$ accumulation interval, the plot of the mean miss distances does not have the simple and straightforward interpretation as in the previous example.

		Methods		
# ΔV		RS	DIR	SC
$m = 5$	$\bar{J}(mm/s)$	2.057	1.956	**1.728**
	$\mathcal{P}_i^{max}$	2.01e-12	2.70e-10	2.23e-06
	$\tilde{P}_c$	0	0	3.84e-6
$m = 10$	$\bar{J}(mm/s)$	1.213	1.150	**1.025**
	$\mathcal{P}_i^{max}$	1.61e-12	2.99e-10	4.04e-06
	$\tilde{P}_c$	0	0	6.53e-6
$m = 20$	$\bar{J}(mm/s)$	1.126	**1.067**	1.347
	$\mathcal{P}_i^{max}$	8.87e-13	2.54e-10	2.03e-23
	$\tilde{P}_c$	0	0	0

Table 2: Test case 2 - Fuel consumption, maximal instantaneous collision probability and MC cumulative collision probability for 5, 10 and 20 maneuvers respectively.

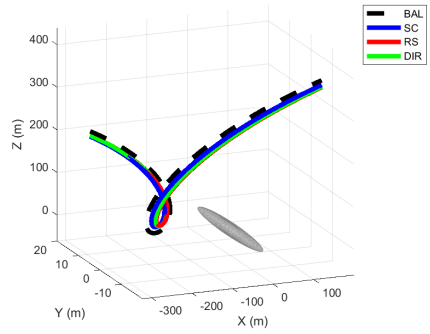

Figure 4: Test case 2 - mean relative trajectories and forbidden region (in grey) for $m = 10$.

5 Conclusion

The problem of efficient impulsive CAM design for the possible encounter between an active spacecraft and an orbital debris, already studied in [8], is considered in this paper for the specific class of long-term encounters. It is formulated as a joint chance-constrained optimization problem, which is difficult to solve without additional simplifications. Two different strategies are presented: a direct convex relaxation and a scenario approach. Then, they are compared to the risk selection method of [8] on two standard long-term encounters test cases from [17]. From these preliminary studies, it appears

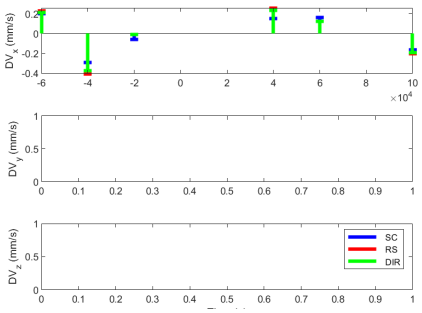

Figure 5: Test case 2 - ΔV components vs firing times for $m = 10$.

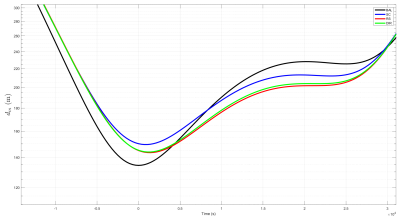

Figure 6: Test case 2 - Distances between the mean relative trajectories and the origin of the hardbody for $m = 10$.

that both proposed approaches are competitive with the state-of-the-art methods dealing with long-term encounters. The scenario-based approach provides an interesting alternative, in terms of tuning parameters (ε and β) and, despite being more computationally intensive, it lays ground for future applications of scenario-based methods to spacecraft collision avoidance.

These results have to be consolidated and confirmed on more challenging and realistic examples of long-term conjunctions. A theoretical analysis of the probabilistic guarantees of the present scenario-base method compared to the ones obtained by using the conservative reformulation given by the Average Value-at-Risk would definitely be an interesting future direction of research.

References

[1] D. B. Spencer, M. E. Sorge, and M. A. Skinner, "Establishing "norms of behavior" for satellite collision avoidance maneuver planning," *Journal of Space Safety Engineering*, vol. 11, no. 1, pp. 120–126, 2024.

[2] M. Mejía-Kaiser, "Space debris mitigation guidelines of the committee on the peaceful uses of outer space, united nations," in *The Geostationary Ring*. Brill Nijhoff, 2020, pp. 390–394.

[3] F. K. Chan, *Spacecraft collision probability*. American Institute of Aeronautics and Astronautics, Inc., 2008.

[4] J. Dolado-Perez, P. Legendre, R. Garmier, B. Revelin, and X. Pena, "Satellite Collision Probability Computation for Long Term Encounters," *Advanced Astronomical Society / American Institute of Aeronautics and Astronautics Astrodynamics Specialist Conference*, vol. 142, 2011.

[5] G. Krier, "Satellite Collision Probability for Long-term Encounters and Arbitrary Primary Satellite Shape," in *Proceedings of the 7th European Conference on Space Debris*, 2017.

[6] S. Alfano, "Review of conjunction probability methods for short-term encounters (aas 07-148)," *Advances in the Astronautical Sciences*, vol. 127, no. 1, 2007.

[7] J. B. Mueller and R. Larsson, "Collision avoidance maneuver planning with robust optimization," in *7th International ESA Conference on Guidance, Navigation and Control Systems*, 2008.

[8] R. Serra, D. Arzelier, M. Joldes, and A. Rondepierre, "Probabilistic collision avoidance for long-term space encounters via risk selection," in *Advances in Aerospace Guidance, Navigation and Control*. Springer, 2015, pp. 679–698.

[9] G. Calafiore and M. C. Campi, "Uncertain convex programs: randomized solutions and confidence levels," *Mathematical Programming*, vol. 102, pp. 25–46, 2005.

[10] W. Fehse, *Automated rendezvous and docking of spacecraft*. Cambridge university press, 2003, vol. 16.

[11] J. Tschauner and P. Hempel, "Optimale beschleunigungsprogramme für das rendezvous-manöver," *Astronautica Acta*, vol. 10, pp. 296–307, 1964.

[12] K. Yamanaka and F. Ankersen, "New state transition matrix for relative motion on an arbitrary elliptical orbit," *Journal of guidance, control, and dynamics*, vol. 25, no. 1, pp. 60–66, 2002.

[13] G. Slater, S. Byram, and T. Williams, "Collision avoidance for satellites in formation flight," *Journal of Guidance, Control and Dynamics*, vol. 29, no. 5, September-October 2006.

[14] M. Leomanni, G. Bianchini, A. Garulli, A. Giannitrapani, and R. Quartullo, "Sum-of-norms model predictive control for spacecraft maneuvering," *IEEE Control Systems Letters*, vol. 3, no. 3, pp. 649–654, 2019.

[15] R. Bevilacqua and M. Romano, "Fuel-optimal spacecraft rendezvous with hybrid on-off continuous and impulsive thrust," *Journal of Guidance, Control and Dynamics*, vol. 30, no. 4, July-August 2007.

[16] V. T. Coppola *et al.*, "Including velocity uncertainty in the probability of collision between space objects," in *AAS/AIAA Spaceflight Mechanics Meeting*, 2012.

[17] S. Alfano, "Satellite conjunction monte carlo analysis," *Adv. Astronaut. Sci*, vol. 134, pp. 2007–2024, 2009.

[18] R. Serra, D. Arzelier, M. Joldes, J.-B. Lasserre, A. Rondepierre, and B. Salvy, "Fast and accurate computation of orbital collision probability for short-term encounters," *Journal of Guidance, Control, and Dynamics*, vol. 39, no. 5, pp. 1009–1021, 2016.

[19] P. Gurfil, *Modern astrodynamics*. Elsevier, 2006.

[20] A. Shapiro, D. Dentcheva, and A. Ruszczyński, *Stochastic programming - Modeling and Theory*. Philadelphia, PA, USA: SIAM, 2009.

[21] G. C. Calafiore and M. C. Campi, "The scenario approach to robust control design," *IEEE Transactions on automatic control*, vol. 51, no. 5, pp. 742–753, 2006.

[22] U. E. Núñez Garzón and E. G. Lightsey, "Relating collision probability and separation indicators in spacecraft formation collision risk analysis," *Journal of Guidance, Control, and Dynamics*, vol. 45, no. 3, pp. 517–532, 2022.

[23] M. Masson, D. Arzelier, F. Bréhard, M. Joldes, and B. Salvy, "Fast and reliable computation of the instantaneous orbital collision probability," *HAL Open Science*, vol. 1, pp. 1–38, 2023.

[24] S. Zhang, T. Fu, D. Chen, and H. Cao, "Satellite instantaneous collision probability computation using equivalent volume cuboids," *Journal of Guidance, Control, and Dynamics*, vol. 43, no. 9, pp. 1757–1763, 2020.

[25] L. Blackmore, H. Li, and B. Williams, "A probabilistic approach to optimal robust path planning with obstacles," in *Proceedings of the American Control Conference*. IEEE, 2006, pp. 7–pp.

[26] R. Henrion, "Structural properties of linear probabilistic constraints," *Optimization: a journal of mathematical programming and operations research*, vol. 56, no. 4, pp. 425–440, 2007.

[27] T. Lew, R. Bonalli, and M. Pavone, "Risk-Averse Trajectory Optimization via Sample Average Approximation," Sep. 2023. [Online]. Available: http://arxiv.org/abs/2307.03167

[28] X. Wang, Y. Li, X. Zhang, R. Zhang, and D. Yang, "Model predictive control for close-proximity maneuvering of spacecraft with adaptive convexification of collision avoidance constraints," *Advances in Space Research*, vol. 71, no. 1, pp. 477–491, Jan. 2023.

[29] H. Park, S. Di Cairano, and I. Kolmanovsky, "Model predictive control for spacecraft rendezvous and docking with a rotating/tumbling platform and for debris avoidance," in *Proceedings of the 2011 American Control Conference*, 2011.